Precious metal core-shell spindles

X. Xu and M.B. Cortie

Institute for Nanoscale Technology, University of Technology Sydney, Australia

Key words: silver nanoparticles, hematite, optical properties, core-shell

PO Box 123, Broadway, NSW 2007, Australia

Tel +61 2 9514 2208, Fax +61 2 95147553

Email: Michael.cortie@uts.edu.au

Abstract

A simplified method to produce spindle-shaped particles with a hematite core and a silica shell is described. The silica shell can, in turn, serve as the substrate for an outer coating of Ag or Au nanoparticles. The resulting multi-layer core-shell particles display a flexible optical extinction spectrum, due primarily to the sensitivity of their plasmon resonance to the morphology of the precious metal outer coating.

Xiaoda Xu and M.B. Cortie *

J. Phys. Chem. C

Silver and gold nanoshells on spindle-shaped particles

The deposition of silver or gold onto spindle-shaped cores produces particles with distinctive optical properties. A silica interlayer between core and shell facilitates attachment of the precious metal. The morphology of the metal coating can be controlled by adjustment of the deposition conditions, and controls the optical extinction characteristics.

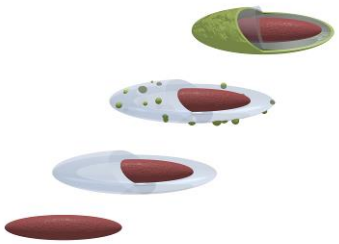

Introduction

Precious metal nanoparticles such as gold or silver nanorods[1,2], nanoshells[3], and nanocaps[4,5] have attracted considerable attention recently. These particles are of particular interest for potential or actual optical applications due to their unique surface plasmon resonances[6]. The nature and position of the resonances is directly determined by the geometry and composition of the particles, allowing considerable tunability in optical response. In the present paper we explore and extend understanding of a very recently developed new design of core-shell particle: the 'nanorice'[7]. This interesting particle has properties intermediate between those of nanorods and nanoshells.

Gold and silver *nanoshells* of less than about 100 nm diameter have a single, strongly developed, extinction peak that can be tuned across the visible and infrared regions of the spectrum by adjusting the ratio of shell thickness to outer diameter of particle[8,9]. While various methods of synthesis have been reported, the mainstream route, as pioneered by the Halas group in the USA, is to use silica nanoparticles as cores, functionalize the surface of the cores with a reagent such as aminopropyltriethoxysilane, attach colloidal gold seeds, and then grow the seeds to coalescence[10]. There has been particular interest in using these particles in medical applications, and experimentation along these lines is well advanced[11-15].

Gold *nanorods* of less than about 150 nm length have two surface plasmon resonance peaks, one due to a longitudinal plasmon and the other to transverse plasmons. The position of the longitudinal peak may be adjusted by control of the aspect ratio[1,2] and morphology[16,17]. This feature may be exploited in the application of surface plasmons in spectrally selective coatings[18], metal-enhanced fluorescence[19], Raman spectroscopy[20], and photothermal medical treatments[21,22]. So far, almost all the methods of making such particles by wet chemistry use a surfactant such as cetyltetra-ammonium bromide (CTAB) and gold 'seed' particles[23]. The surfactant acts as a "soft template"[24] to nucleate the shape and to form a protecting layer to stabilize the particles[25]. Unfortunately, the CTAB molecules are strongly attached to the surface of the gold nanorods, and are difficult to remove by washing[18]. Such particles cannot be readily re-dispersed organic solvents[26], which would

be a desirable attribute for many of the proposed applications[26]. Complicated procedures, such as multi-step polyelectrolytic coating[26,27], are currently required to replace the CTAB with another surfactant before the particles can be stabilized in, for example, ethanol solution.

A 'nanorice' particle is elongated like a nanorod but comprised of a precious metal coating on a dielectric core. The plasmonic properties of this hybrid morphology are intermediate in nature between those of spherical nanoshells and of nanorods[7]. As for nanoshells (for example ref.[28]), a sparse coating of precious metal particles on the core, as opposed to a continuous shell, may also be readily obtained if desired, providing a convenient way to control the dipole-dipole interactions of closely spaced precious metal nanoparticles. In general, dipole-dipole interactions red-shift and broaden the plasmon resonance.[28-30]. This has potential application in, for example, spectrally selective coatings for windows[31]. The 'nanorice' concept offers a uniquely flexible platform to blend all of the flexibility of nanorods, nanoshells and dipole-dipole interactions into a single product, and potentially offers the most flexible optical gamut of any known particle. (Note that the term 'nano-rice' has also subsequently been applied in the literature[32] to elongated nanoparticles that are comprised of a single material. This usage of the word appears inconsistent with the intent of the founding definition[7] of Wang *et al*.)

A basic problem when attempting to prepare nanorice (or indeed any core-shell particle) by wet chemical means is to achieve nucleation and growth of the plasmonically-active gold or silver shell on the dielectric core. This is because surface energy considerations generally inhibit the attachment of Au or Ag nuclei to candidate dielectric core materials. (This problem can be overcome by synthesizing the particles in a high temperature, highly reducing, organic environment, e.g.[33], but this is not for the faint-hearted.) In the original[7] synthesis of the nanorice particles, the problem was solved by functionalizing the surface of the Fe_2O_3 core with 3-aminopropyl trimethoxysilane (APTMS), so that colloidal Au seed crystals could be attached. The gold seeds were then grown to form a continuous shell. Similarly, the silane molecules serve as an interlayer between the core material and the gold seeds. The formation of a covalent bond between the core particle and the

gold/silver seed is an essential attribute of this process. However, in the present work we demonstrate an alternative, possibly more convenient, way to attach gold or silver particles to an oxide substrate, and we analyze the factors that influence the microstructure and optical properties of the resulting structures.

Experimental

The basic principle is to facilitate the attachment of the precious metal by first coating the dielectric core particle with a smooth coating of SiO_2 using the Stöber method[34]. The shape, and many other properties, of the core particles are preserved during this process. Actually, the idea of encapsulating nanoparticles with a SiO_2 overlayer is not new, having been pioneered by the Mulvaney group (if not others) in the late 1990s[35-38]. Furthermore, deposition of silver or gold on silica is a well-known technology[39,40]. For example, silver and gold films have been applied on glass or silica surfaces electrolessly, for example as reflective mirrors[41] or as prototype solar-blocking glazing[31].

Materials

Ferric chloride hexahydrate ($FeCl_3.6H_2O$), potassium dihydrogen phosphate (KH_2PO_4), tetraethyl orthosilicate (TEOS), 2-propanol, concentrated ammonium hydroxide solution (~ 17 M), stannous chloride dihydrate ($SnCl_2.2H_2O$), hydrochloric acid (HCl), silver nitrate ($AgNO_3$) and formaldehyde (CH_2O) were ordered from Sigma-Aldrich. All chemicals were reagent grade and used without further purification. All water used was purified by Milli Q system and had an electrical resistance of 18.4 MΩ/cm.

Procedure for making spindle-shaped, silica-coated hematite nanoparticles

a. Hematite spindles

The hematite particles were synthesized through hydrolysis of ferric chloride hexahydrate, a procedure reported by Ohmori *et al*.[42]. The method is briefly described here: 150 mL of aqueous solution containing 20 mM $FeCl_3$ and 0.4 mM KH_2PO_4 was aged at 100^{o}C for 48 hours. The orange slurry obtained was then centrifuged three times to remove the excess ions. The particles were re-dispersed in 20 mL water. The product contained ~20 mg/mL of hematite particles.

b. Silica coating

Silica-coated hematite particles were prepared with the modified Stöber method by controlled hydrolysis of silane in the presence of alcohol[43]. Between 2.0 and 5.0 mL (~40 to 100 mg) hematite colloid was mixed with 50 mL concentrated ammonium hydroxide (~ 17 M), 50 mL H_2O and 200 mL 2-propanol. Then, 1.0 mL TEOS was added with vigorous stirring. The mixture was then held at 40^{o}C in a water bath for various times. The colloid was purified by centrifuging twice, and then re-dispersed in 30 mL water. The colloid contained 0.1 ~ 0.3 mg/mL of silica-coated hematite particles. The thickness of shell can be controlled by varying the ratio of hematite particles and TEOS introduced and/or by varying the reaction time

Procedure for deposition of silver and gold

a. Stannous chloride pre-treatment

The silica-coated hematite particles were ‘sensitized’ with stannous chloride, a treatment that facilitates the subsequent nucleation of precious metal onto an otherwise inert substrate, e.g.[40] Due to the large specific area of the nanoparticles, a comparatively large amount of $SnCl_2$ must be used to obtain reasonable coverage. Typically, 3 mg of silica-coated hematite (10 mL colloid as

prepared) was transferred into 20 mL of 0.2% $SnCl_2.2H_2O$ aqueous solution. The pH of the solution was adjusted to 1.5~3 by 1 M HCl to avoid hydrolysis and oxidation of $SnCl_2$. The mixture was magnetically stirred for an hour before it was centrifuged twice to remove the excess of $SnCl_2$ and other ions in the solution. The particles that had been pretreated with $SnCl_2$ were redispersed in 15 mL of water. Therefore, the resulting colloid contained 0.2 mg/mL silica-coated hematite particles.

b. Silver deposition

The solution used to deposit Ag onto the silica-coated hematite particles had 0.25 ~ 2 mM $AgNO_3$, 0.23 M NH_4OH solution and 6 ~ 13 mM CH_2O. Usually, 0.03 ~ 0.2 mg of Sn-activated particles were introduced into 5 mL of such solution. The deposition solution stayed stable during the reaction since it contained a high concentration of ammonia. Once contacted with the colloid, the self-catalyzed reaction was essentially finished within 20 minutes. The entire process is schematically illustrated in **Figure 1**.

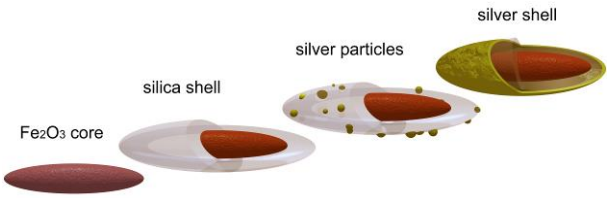

Figure 1. Schematic illustration of the process for making a spindle-shaped, silver nano-shell with a hematite core.

c. Gold deposition

Sn-activated silica-coated hematite particles were mixed with solution containing 0.4 mM $HAuCl_4$ and 6 to 13 mM CH_2O. The pH of $HAuCl_4$ solution was pre-adjusted to ~10 by 0.1 M K_2CO_3 [44].

Materials characterization

The morphologies of the samples were studied in a Zeiss Supra 55VP LEO scanning electron microscope at 20 KV. The novel in-lens detector of the instrument provides 2 nm spatial resolution and excellent contrast of multi-layer nanostructures. UV-visible absorption spectra were obtained from a Shimadzu 1240 mini UV-Visible absorption spectrometer in the wavelength range 300 ~ 1100 nm. The spectra were obtained at scanning speed of 600 nm/min with its spectral bandwidth (SBW) of 5 nm. X-ray Photoelectron Spectroscopy (XPS) was utilized to determine the chemical composition of the particles' surface. The colloidal samples were dried in a desiccator overnight before being measured in the XPS instrument. XPS spectra were recorded by using Al (Kα) radiation (1486.6 eV) at 50 eV. The datasets obtained were calibrated with the carbon peak (285 eV) to counteract the effect of static charge. The crystal structure of the core-shell composites was characterized with a Siemens Z6000 X-ray diffractometer using a copper target at 40 kV. The samples were scanned from 15~85^{o} (2θ) with a step size of 0.02^{o}.

Simulation of optical properties

Some insight into the optical properties of the Ag-coated spindles was obtained by simulations using DDSCAT, a code based on the discrete dipole approximation[45,46]. Although computationally intensive, this code will give usable results for arbitrary-shaped targets provided that the dipole volume used is small enough. Unfortunately, the total volume of the Fe_2O_3 core, the silica shell and the Ag outer coating was too great to satisfy this criterion within the memory limitations of the computers used, and also because the length of time taken for DDSCAT to converge depends on the third power of the number of dipoles used[47]. To render the problem tractable, only the Ag portion of the particle was simulated. We submit that this is acceptable, since it is only the Ag portion that undergoes the plasmon resonance in the visible part of the spectrum, with the remainder of the particle only serving to red-shift the plasmon phenomena somewhat. A dipole volume of about 18 nm^3 was thus obtained, sufficiently small to provide an indication of the general trends. The

extinction efficiencies shown are the average of a transverse and longitudinal orientation of each target.

Results

Evolution of particle morphology

a. Morphology of hematite spindle particles

The hematite particles prepared by controlled hydrolysis are shown in

Figure 2. The particles are generally 200~250 nm in length and 50~80 nm in width. SEM imaging at higher magnifications revealed that the particles were actually aggregations of smaller clusters (

Figure 2(b)). The rough substrate provides an ideal surface for keying in the subsequent silica coating.

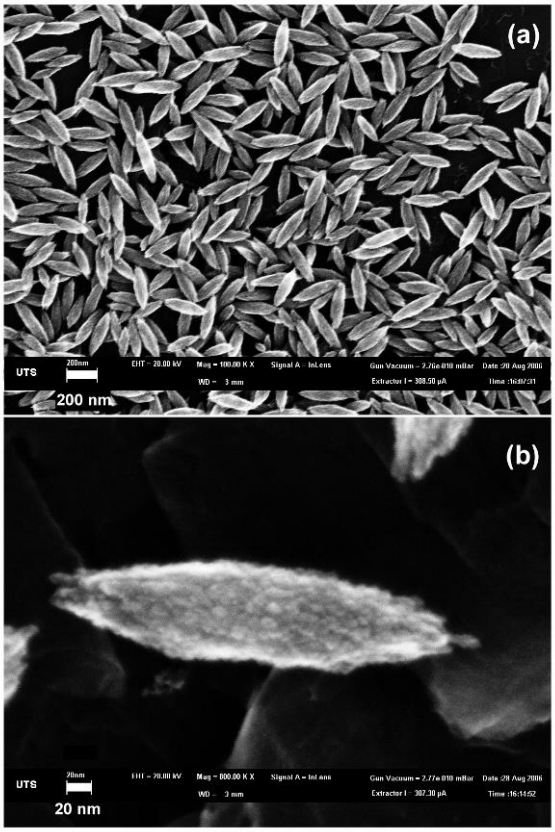

Figure 2. Hematite spindles synthesized by controlled hydrolysis of $FeCl_3$

b. Morphology of silica-coated hematite spindles

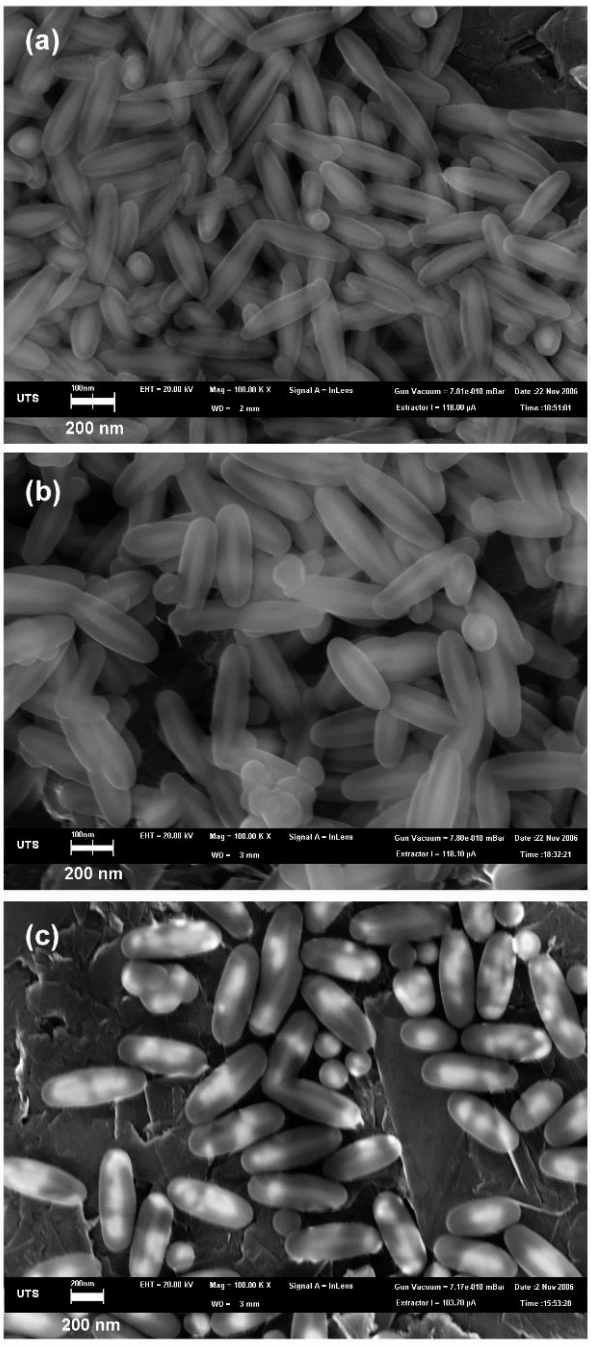

Figure 3. Fe_2O_3/SiO_2 core-shell structures with varying thickness of SiO_2. (a) 0.6 mg/mL hematite, 5 μl/mL TEOS, (b) 0.3 mg/mL hematite, 5 μl/mL TEOS, (c) 0.15 mg/mL hematite, 3.3 μl/mL TEOS; all aged in solution for 15 hours.

The thickness of the silica coating (**Figure 3**) was controlled by the ratio of the particles and TEOS in the growth solution. In this study, the thickness of silica was controlled within the range from 20 ~ 60 nm. The spindle shape of the hematite particles was preserved in the process, but the surface become much smoother, and the aspect ratio of the particles was decreased.

An examination of XPS spectra confirmed that, as expected, silica was deposited on the hematite surface from the TEOS solution. As the silica shell increased in thickness the iron peaks in the spectra diminished while the silica peaks became prominent (Figure 4). This is because XPS is a surface-sensitive technique; any photoelectron that originated from more than about 5 nm under the surface does not possess sufficient kinetic energy to be detected.

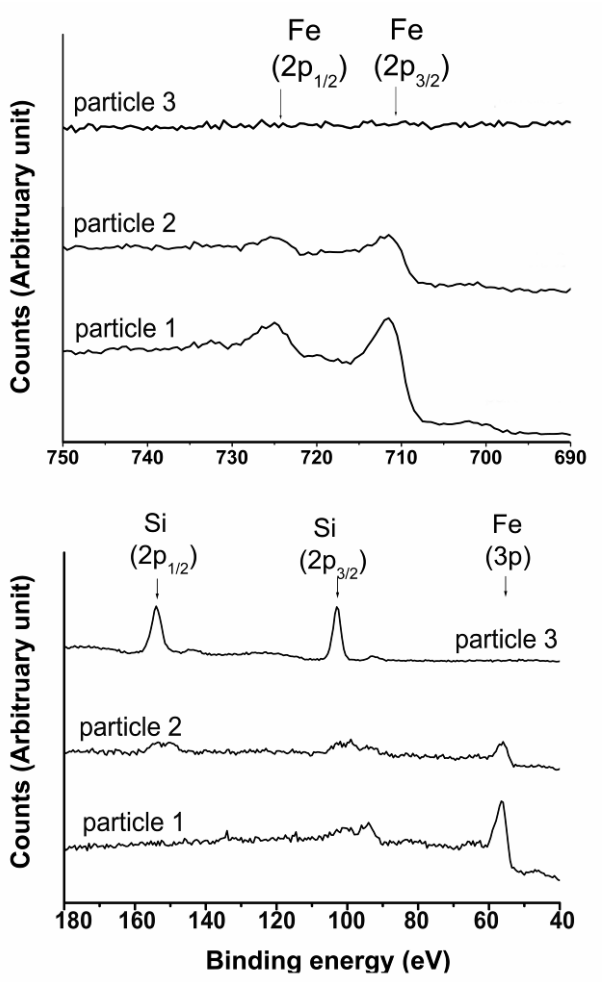

Figure 4 XPS spectra showing the disappearance of Fe peaks and the appearance of Si peaks as the shell of silica formed. Particle 1 corresponds to a naked hematite particle, particle 2 is

hematite coated with a thin coating of SiO_2 (Figure 3(a)), and particle 3 is hematite coated with a thick layer of SiO_2 (Figure 3(c)).

The XRD patterns (Figure 5) indicate that the spindle-shaped hematite particles produced by controlled hydrolysis of $FeCl_3$ are α–Fe_2O_3. However, no silica peaks were evident in the XRD data sets of samples that had been coated by the Stöber method. The broad peak shown in the spectrum around 15~30^o suggests that silica shell could be either amorphous or nano-crystalline [48].

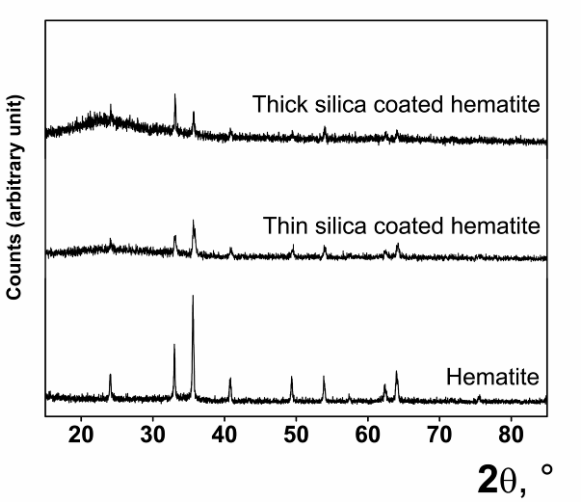

Figure 5 XRD patterns of the core particles, showing the disappearance of the peaks due to hematite as the silica shell thickened. The silica shell itself is evidently nanocrystalline or amorphous.

c. The particles after Sn pre-treatment

The morphology of particles before and after Sn activation is shown in Figure 6. In these high resolution SEM images, grains of 1 to 5 nm size of a new substance are observed on the surface of particles after treatment with $SnCl_2$. These grains are probably comprised of some tin (II) compound, and are evidently the nuclei for subsequent deposition of the precious metal. No change in the optical properties occurred during the pre-treatment process.

The XPS spectra confirmed the existence of the tin on the surface of the particles after the $SnCl_2$ pretreatment. The $SnCl_2$ pretreated samples had been washed four times by centrifugation to ensure there was no excess $SnCl_2$ in the dispersion.

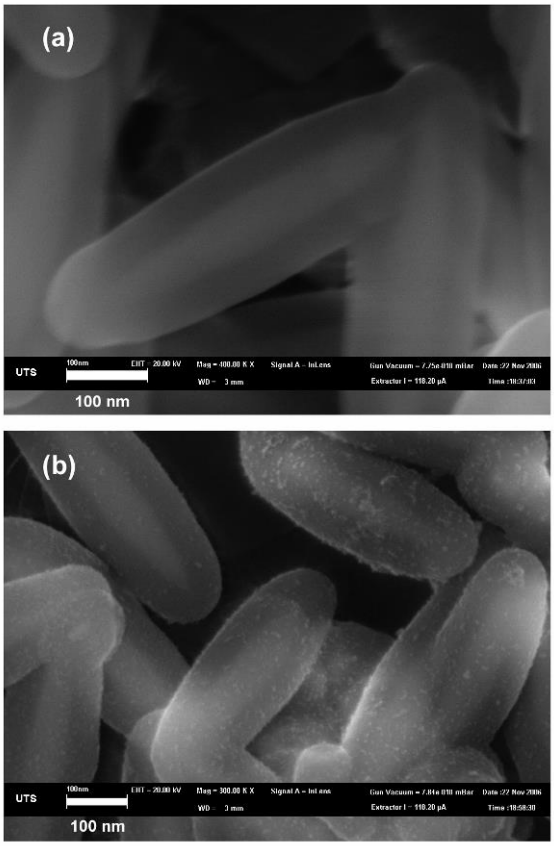

Figure 6 Particles before and after treatment with $SnCl_2$ solution, (a) before $SnCl_2$ treatment; (b) after $SnCl_2$ treatment.

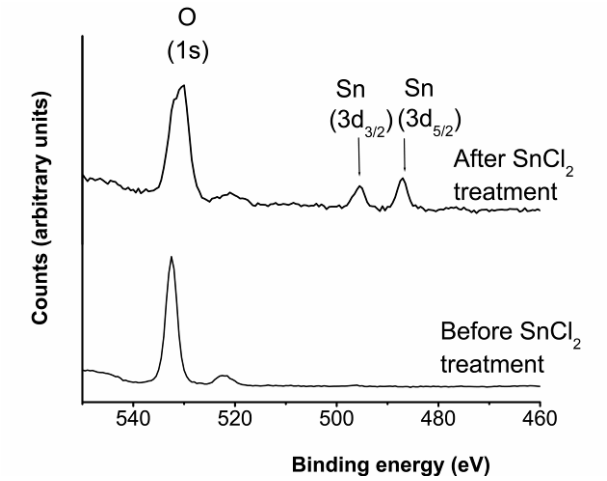

Figure 7 XPS spectra showing evidence of Sn absorption onto the silica shell.

d. Morphology of silver coated spindle particles

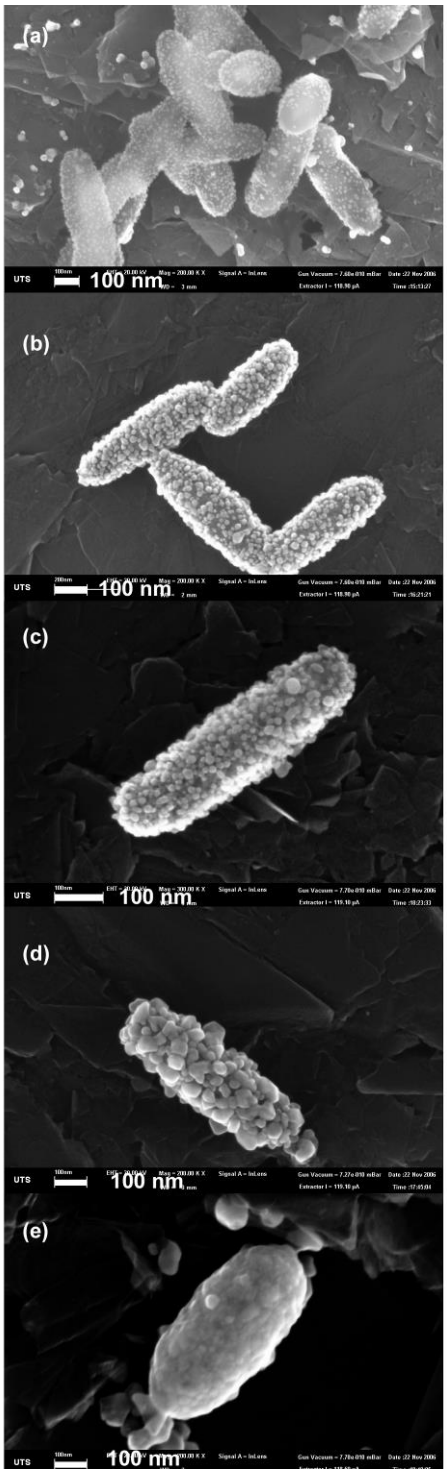

Figure 8 $Fe_2O_3/SiO_2/Ag$ multi-layer core-shell particles with increasing coverage of Ag, (a) 0.12 mg/mL hematite, 0.25 mM Ag^+ stop once color changed; (b) 0.12 mg/mL hematite, 0.25 mM Ag^+; (c) 0.12 mg/mL hematite, 1 mM Ag^+, (d) 0.12 mg/mL hematite, 1 mM Ag^+ redeposit 3 time, (e) 0.01 mg/mL hematite, 2 mM Ag^+.

.

The morphologies of $Fe_2O_3/SiO_2/Ag$ core-shell structures prepared with varying proportions of reactants are shown in Figure 8. At low concentrations of Ag, isolated particles of Ag ranging between 2 and 5 nm in size were deposited on the SiO_2 surface coating (Figure 8a.). The Ag particles for this sample show a narrow size distribution. When a larger amount of Ag was available, nucleation continued for some time, with the particles that formed first growing to a larger size. This inevitably resulted in a wide distribution of particle sizes (Figure 8b (b, c)), with the central tendency being in the 10 to 20 nm range. However, the silica surface was not yet fully covered by Ag. Further increase of Ag concentration resulted in the formation of a contiguous coverage of Ag nanoparticles (Figure 8 d.), which were granular and un-coalesced in nature. Nevertheless, the packing density of the Ag particles in this stage is so high that the surface of the Fe_2O_3/SiO_2 composite particle is fully covered. The size of these particles also increased somewhat from 10 to 20 nm, to 15 to 30 nm. Finally, a continuous shell structure was observed in solutions of very high Ag content. In this case, the coating of Ag deposited on the SiO_2 surface appeared uniform and relatively smooth. (Figure 8 e). There were two practical problems associated with the production of the last type of particle: firstly, yield of the composite particles was low due to very low concentration of hematite particles in the solution, and secondly the solution was unstable and susceptible to auto-catalytic self-decomposition. When this occurred free Ag was also precipitated, which rendered isolation of the particles difficult.

Examination of the images revealed that the size of the particles increased with the silver concentration. At first sight this might be unexpected for a nucleation-and-growth reaction. It is generally observed in such reactions that greater driving force and faster reaction rate tends to produce more nuclei and a smaller final particle size, which would also be the preferred situation when attempting to produce a thin, continuous coating of Ag. In the present instance, however, the large specific surface area (of the order of 10 m^2/g)[49] has the consequence that nucleation sites are abundant. Therefore, the rate of nucleation is not a restriction. It is likely that Ag nuclei are formed rapidly once the particles are contacted with the Ag-containing solution. The particle size effect is

therefore likely to be due simply to depletion of the available Ag^+, with larger particles growing where more Ag^+ was available.

Effect of tin sensitization

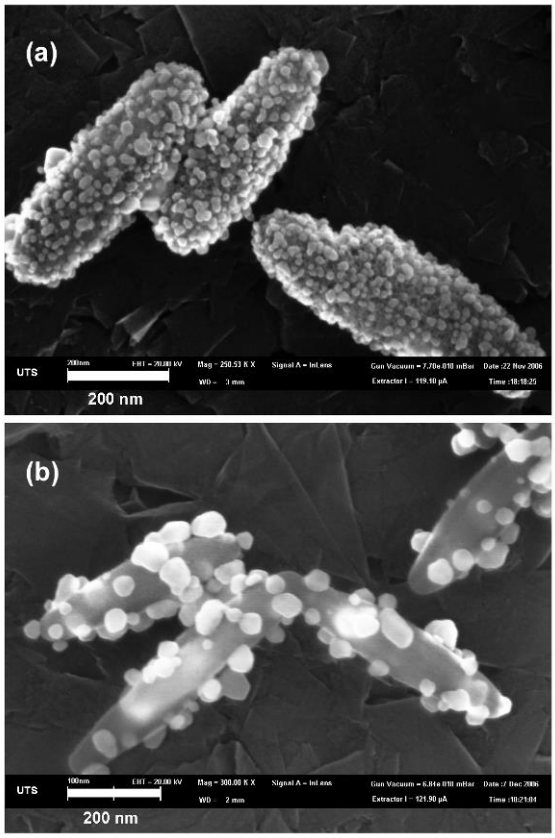

Figure 9 Effect of aging on the quality of silver coatings, (a) $SnCl_2$ pretreatment followed immediately by deposition of Ag, (b) $SnCl_2$ pretreatment followed by a 48 h in air, then deposition of Ag.

It was found that the nature of the tin pre-treatment had a large effect on the morphology of the Ag particles. Two typical morphologies induced by different tin pre-treatment processes, but with otherwise identical coating conditions, are indicated in Figure 9. In Figure 9(a), the normal tin pre-treatment process was applied, in which the silver deposition process was initiated immediately following the tin pre-treatment. In Figure 9 (b), the pre-treated samples were exposed to air for 48

hours, after which the same Ag deposition process was applied. It is clear that a prompt deposition of Ag resulted in a smaller particle size and narrower size distribution. This is essential to make a thin, prolate silver shell structure. A delay in Ag deposition, however, led to precipitation of fewer and larger Ag nanoparticles.

Tin pre-treatment is a process in which absorption of Sn^{2+} ion occurs on the surface of the silica according to Equation (1), following which silver ions are deposited as shown in equation (2):

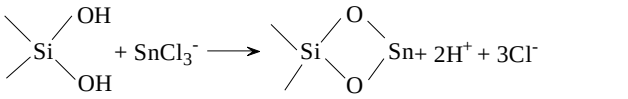

(1)

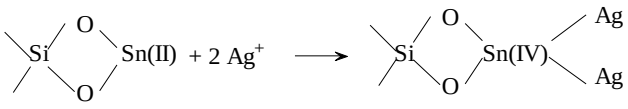

(2)

These are the sites at which Ag or Au nanoparticles subsequently nucleate. Once the nuclei are in place, further reduction and deposition proceeds auto-catalytically[50]. However, tin(II) is vulnerable to oxidation, which causes the density of nucleation sites on the surface to drop with time. If this occurs then the reduction reaction occurs on far fewer sites, which results in a wide size distribution and large average particle size. The deposition of Ag on the silica surfaces evidently follows the Volmer-Weber mechanism of film growth[51]. In this model separate, three-dimensional islands (nanoparticles) are grown on the substrate in the initial stage before these isolated islands coalesce to form continuous networks. Therefore, the size of these isolated nanoparticles during the coalescence is critical for the percolation thickness, which in turn largely determines the optical properties of the Ag film. Usually, a high density of nuclei tends to produce smaller Ag particles. Therefore, oxidation of the surfaces that had been pre-treated with Sn was disadvantageous for the subsequent formation of a continuous film of Ag.

Au-coated spindles

The template deposition method provides a universal way to engineer an anisotropic, metallic multi-layered shell structure. For example, a Fe_2O_3/SiO_2/Au core-shell structure can also be made by this method. The gold-coated spindles (so-called gold nanorice[7]) are prepared by deposition of gold nanoparticles on the silica-coated spindle hematite cores. From the high resolution SEM image it can be seen that some particles started to coalesce even before the silica surface had been fully covered by the gold (Figure 10).

Figure 10 An example of a Fe_2O_3/SiO_2/Au multi-layer core-shell structure

Optical properties of particles

The optical extinction spectra are directly linked to the morphologies of these multi-layer nanostructures. The effect of the density of Ag particles is shown in Figure 11. The examples shown extend from sparse coatings of Ag particles (Figure 11, line corresponding to 3.5 mM Fe_2O_3) to samples with a continuous Ag film (Figure 11, line corresponding to 0.06 mM Fe_2O_3). Although the silica coating and tin pre-treatment caused no change in optical properties of the hematite, it is clear that the deposition of silver particles on the silica surface had a marked effect. The surface plasmon peak of individual silver nanospheres is prominent in samples containing a greater ratio of Fe_2O_3 to Ag. In these instances neither the silver particle-to-particle interaction nor the silver shell

contributes significantly to the absorption peak. However, a second peak emerges and shifts to longer wavelengths with a further increase of the Ag to Fe_2O_3 ratio, even while the silver surface plasmon peak around 425 nm is still observed. This new peak is evidently related to the increase of the particle density on the surface and/or coalescence of the silver particles to form continuous films.

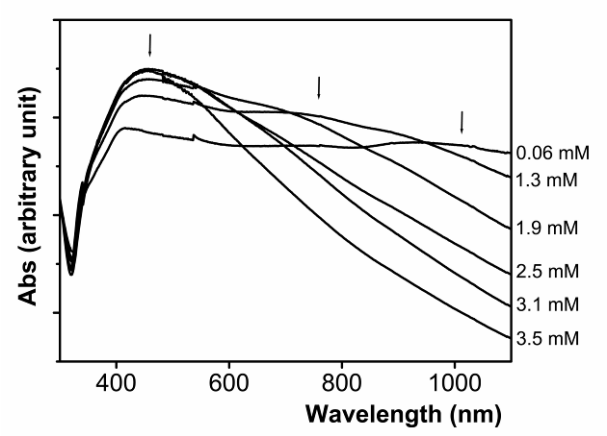

Figure 11 Normalized optical extinction spectra of the $Fe_2O_3/SiO_2/Ag$ nanorice particles, prepared using varying concentrations of Fe_2O_3 (concentration used shown next to each measurement). The progressive red shift of the second plasmon resonance peak as the ratio of Ag to Fe_2O_3 increases is indicated with the arrows.

The size of the Ag particles also has a profound effect, Figure 12. For a sparse coverage of fine Ag particles (Figure 12a), the spectrum shows a strong single surface plasmon resonance peak around 425 nm (Figure 12c, line (a)). However, when a coarse texture of silver particles was developed (Figure 12b) the spectrum (Figure 12c, line (b)) is substantially different, with a broad absorption peak ranging from 500 nm to 700 nm, even while the single-particle surface plasmon absorption of 425 nm is still observed. The broad absorption of the particles shown in Figure 12b results from two factors: firstly, the formation of large silver particles (~50 nm) red-shifts and broadens the surface plasmon peak, secondly, the higher packing density of Ag particles on the silica surface results in a smaller inter-particle space, which cause particle-to-particle interactions.

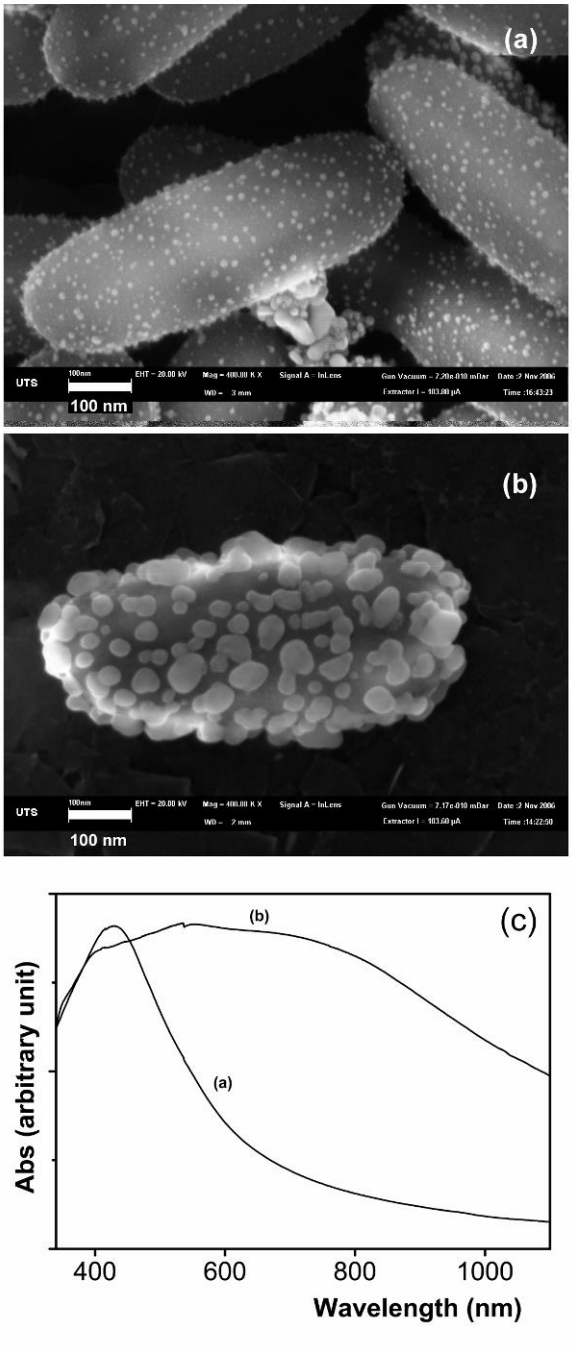

Figure 12 Effect of particle size. (a) Isolated silver particles – low coverage 0.05mg/mL hematite, 2mM Ag^{+}; (b) Isolated silver particles – high coverage 0.05mg/mL hematite, 2mM Ag^{+}. (c) Spectra of hematite particles coated with Ag as shown in (a) and (b).

Similar trends are observed for the case of gold coatings, Figure 13. The coverage of Au on the spindles increases as the ratio of Fe_2O_3 to Au is decreased. The result is a more comprehensive coverage of the core with Au and, as for Ag, a red-shifting and broadening of the extinction peak.

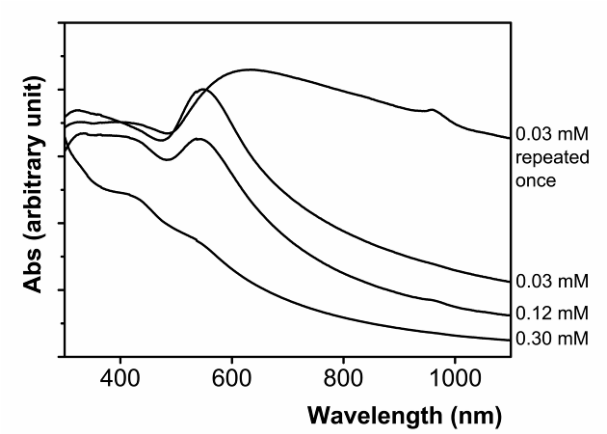

Figure 13 Optical extinction spectra of the $Fe_2O_3/SiO_2/Au$ particles prepared using varying concentrations of Fe_2O_3 (shown alongside data for each measurement). The absorption of the 0.30 mM Fe_2O_3 is essentially that of naked Fe_2O_3/SiO_2 spindles.

Discussion

The broadening of the peaks in the optical extinction spectra are obviously associated with the development of a semi-continuous coating of precious metal nanoparticles. This is also quite evident from the numerical simulations of the extinction spectra, **Figure 14**, which, as mentioned, simplified the particle to its most basic geometry, namely a hollow, spindle-shaped aggregation of silver nanoparticles.

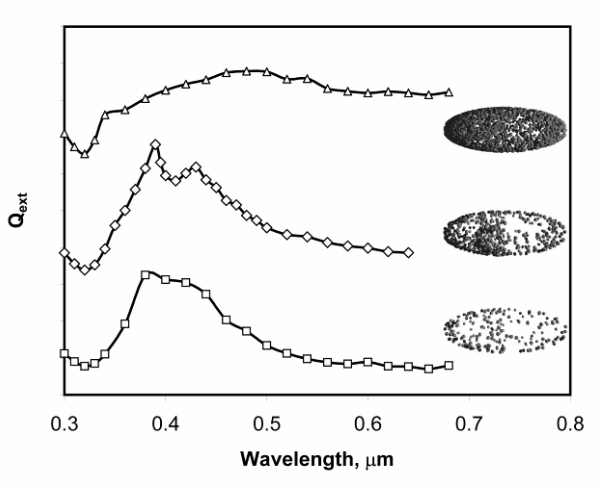

Figure 14. Simulations of the optical extinction spectra of the particular hollow, spindle-shaped aggregations of silver nanoparticles shown. The net effect of increasing the number of Ag nanospheres on the spindle core is to induce a broad, second extinction peak due to particle-particle dipole interactions. This second peak dominates the extinction of the most densely packed structure (top), but both contributions are individually evident on the particle with an intermediate density of Ag (centre).

The templated deposition method provides a means in principle to produce Ag or Au shells, however in some cases the surface or chemical properties of candidate core materials are not suitable for the metal plating solution. The insertion of a silica interlayer ensures that the technique has a more general applicability because it isolates any chemical issues relating to the core particle from the metal solution. This opens up new possibilities in respect of particle compositions, shapes and structures. The unique geometric features of whatever template is used will not be altered by deposition of the silica interlayer. Relatively large seed particles were used for the cores here, however there is no reason in principle why smaller sized seeds could not be used. Examples of interesting possibilities for inert cores include boehmite rods, gibbsite platelets, polystyrene spheres, and copper nanorods, while active core materials such as magnetite nanospheres or vanadium dioxide nanocrystals could be contemplated to yield so-called 'smart' materials with multiple functionalities, e.g.[52].

Conclusion

An improved method for producing anisotropic Ag or Au-coated, spindle-shaped particles is demonstrated in this study. The core of the particle is a hematite spindle that is then coated with a layer of silica. The silica in turn is rendered suitable for the attachment of Ag or Au nanoparticles by an activating treatment with $SnCl_2$. The resulting core-shell structures manifested a plasmonic resonance that could be varied from a single broad peak at ~450 nm through to a broad extinction band spread over 450 to 1000 nm. The details of the optical properties were largely controlled by the morphology and distribution of the attached precious metal nanoparticles which were controlled by the relative proportions of the reactants and the reaction conditions. Lower concentrations of silver were preferable to obtain for thinner, more continuous metallic films, while a coarse texture of the film was developed from more concentrated silver solutions. The silica shells produced by the Stöber method were smooth and continuous, and they preserved the geometric features of the core particle, thereby greatly facilitating the construction of multi-layer, core-shell structures.

Acknowledgement

This work was supported by Australian Research Council grant DP0666689.

References

(1) Murphy, C. J.; Sau, T. K.; Gole, A. M.; Orendorff, C. J.; Gao, J.; Gou, L.; Hunyadi, S. E.; Li, T. *J. Phys. Chem. B* **2005**, *109*, 13857-13870.

(2) Perez-Juste, J.; Pastoriza-Santos, I.; Liz-Marzan, L. M.; Mulvaney, P. *Coordin. Chem. Rev.* **2005**, *249*, 1870-1901.

(3) Oldenburg, S. J.; Jackson, J. B.; Westcott, S. L.; Halas, N. J. *Appl. Phys. Lett.* **1999**, *75*, 2897-2899.

(4) Liu, J.; Maaroof, A. I.; Wieczorek, L.; Cortie, M. B. *Adv. Mater.* **2005**, *17*, 1276 - 1281.

(5) Charnay, C.; Lee, A.; Man, S.; Moran, C. E.; Radloff, C.; Bradley, R. K.; Halas, N. J. *J. Phys. Chem. B* **2003**, *107*, 7327-7333.

(6) Kelly, K. L.; Coronado, E.; Zhao, L. L.; Schatz, G. C. *J. Phys. Chem. B* **2003**, *107*, 668-677.

(7) Wang, H.; Brandl, D. W.; Le, F.; Nordlander, P.; Halas, N. J. *Nano Lett.* **2006**, *6*, 827-832.

(8) Oldenburg, S. J.; Averitt, R. D.; Westcott, S. L.; Halas, N. J. *Chem. Phys. Lett.* **1998**, *288*, 243-247.

(9) Halas, N. *MRS Bull.* **2005**, *30*, 362-367.

(10) Oldenburg, S. J.; Averitt, R. D.; Halas, N. J. Metal nanoshells. *US Patent 6,344,272*, 2002.

(11) Loo, C.; Lin, A.; Hirsch, L.; Lee, M. H.; Barton, J.; Halas, N.; West, J.; Drezek, R. *Technol Cancer Res T* **2004**, *3*, 33-40.

(12) Hirsch, L. R.; Stafford, R. J.; Bankson, J. A.; Sershen, S. R.; Rivera, B.; Price, R. E.; Hazle, J. D.; Halas, N. J.; West, J. L. *Proc. Nat. Acad. Sci. USA* **2003**, *100*, 13549-13554.

(13) O'Neal, D. P.; Hirsch, L. R.; Halas, N. J.; Payne, J. D.; West, J. L. *Cancer Lett.* **2004**, *209*, 171-176.

(14) Hirsch, L.; Gobin, A.; Lowery, A.; F, T.; Drezek, R.; Halas, N.; JL, W. *Annals of Biomedical Engineering* **2006**, *34*, 15-22.

(15) Pissuwan, D.; Valenzuela, S.; Cortie, M. B. *Trends Biotechnol.* **2006**, *24*, 62-67.

(16) Xu, X.; Cortie, M. B. *Adv. Func. Mater.* **2006**, *16*, 2170-2176.

(17) Prescott, S. W.; Mulvaney, P. *J. Appl. Phys.* **2006**, *99*, 123504.

(18) Xu, X.; Gibbons, T.; Cortie, M. B. *Gold Bull.* **2006**, *39*, 156-165.

(19) Aslan, K.; Leonenko, Z.; Lakowicz, J. R.; Geddes, C. D. *J. Phys. Chem. B* **2005**, *109*, 3157-3162.

(20) Orendorff, C. J.; Gearheart, L. A.; Jana, N. R.; Murphy, C. J. *Phys. Chem. Chem. Phys.* **2006**, *8*, 165-170.

(21) El-Sayed, I. H.; Huang, X.; El-Sayed, M. A. *Cancer Lett.* **2006**, *239*, 129-135.

(22) Pissuwan, D.; Valenzuela, S. M.; Killingsworth, M. C.; Xu, X.; Cortie, M. B. *J. Nanoparticle Res.* **2007**, in press, DOI 10.1007/s11051-11007-19212-z.

(23) Jana, N. R.; Gearheart, L. A.; Murphy, C. J. *Chem. Mater.* **2001**, *13*, 2313-2322.

(24) Jana, N. R.; Gearheart, L. A.; Murphy, C. J. *Adv. Mater.* **2001**, *13*, 1389-1393.

(25) Nikoobakht, B.; El-Sayed, M. A. *Chem. Mater.* **2003**, *15*, 1957-1962.

(26) Pastoriza-Santos, I.; Pérez-Juste, J.; Liz-Marzán, L. M. *Chem. Mater.* **2006**, *18*, 2465-2468.

(27) Gole, A.; Murphy, C. J. *Chem. Mater.* **2005**, *17*, 1325-1330.

(28) Peceros, K. E.; Xu, X.; Bulcock, S. R.; Cortie, M. B. *J. Phys. Chem. B* **2005**, *109*, 21516-21520.

(29) Quinten, M.; Kreibig, U. *Surf. Sci.* **1986**, *172*, 557-577.

(30) Ung, T.; Liz-Marzan, L. M.; Mulvaney, P. *Colloids and Surfaces A: Physicochemical and Engineering Aspects* **2002**, *202*, 119-126.

(31) Xu, X.; Stevens, M.; Cortie, M. B. *Chem. Mater.* **2004**, *16*, 2259-2266.

(32) Wiley, B. J.; Chen, Y.; McLellan, J.; Xiong, Y.; Li, Z.-Y.; Ginger, D.; Xia, Y. *Nano Lett.* **2007**, *7*, 1032-1036.

(33) Wang, L.; Luo, J.; Fan, Q.; Suzuki, M.; Suzuki, I. S.; Engelhard, M. H.; Lin, Y.; Kim, N.; Wang, J. Q.; Zhong, C.-J. *J. Phys. Chem. B* **2005**, *109*, 21593-21601.

(34) Stöber, W.; Fink, A.; Bohn, E. *J. Colloid Interface Sci.* **1968**, *26*, 62-69.

(35) Liz-Marzan, L. M.; Giersig, M.; Mulvaney, P. *Langmuir* **1996**, *12*, 4329-4335.

(36) Mulvaney, P. C.; Liz-Marzan, L. M. Stabilized particles and methods of preparation and use therof. *International Patent WO99/21934*, 1999.

(37) Ung, T.; Liz-Marzan, L. M.; Mulvaney, P. *J. Phys. Chem. B* **2001**, *105*, 3441-3452.

(38) Graf, C.; Vossen, D. L. J.; Imhof, A.; Blaadere, A. V. *Langmuir* **2003**, *19*, 6693-6700.

(39) Zhou, C.; Peng, Z.; Jian-hui, Z.; Zhen-lin, W.; Wei-yi, Z.; Nai-ben, M. *Chin. Phys. Lett.* **2003**, *20*, 1369-1371.

(40) Miller, R. G.; Cavitt, R. L. Novel method for the rapid depositon of gold films onto non-metallic substrates at ambient temperatures,. *United States Patent 4,005,229*, 1977.

(41) Laroche, P.; Boulanger, P.; Dauby, C. Silver coated mirror. *United States Patent 6565217B2*, 2003.

(42) Ohmori, M.; Matijevic, E. *J. Colloid Interface Sci.* **1992**, *150*, 594-598.

(43) Ohmori, M.; Matijevic, E. *J. Colloid Interface Sci.* **1993**, *160*, 288-292.

(44) Lim, Y. T.; Park, O. O.; Jung, H.-T. *J. Colloid Interface Sci.* **2003**, *263*, 449-453.

(45) Draine, B. T.; Flatau, P. J. User Guide for the Discrete Dipole Approximation Code DDSCAT 6.1, 2004.

(46) Draine, B. T.; Flatau, P. J. *J. Opt. Soc. Am. A* **1994**, *11*, 1491-1499.

(47) Kooij, E. S.; Poelsema, B. *Phys. Chem. Chem. Phys.* **2006**, *8*, 3349–3357.

(48) Yoshida, H.; Kimura, K.; Inaki, Y.; Hattori, T. *Chem. Commun.* **1997**, 129-130.

(49) Alexander, G. B.; Nadkarni, R. M. Method for electroless plating of ultrafine or colloidal particles and products produced thereby. *United States Patent 4,944,985* US, 1990.

(50) Mallory, G. O.; Hajdu, J. B. *Electroless Plating: Fundamentals and Applications*; American Electroplaters and Surface Finishers Society: Orlando, Florida, 1990.

(51) Kaiser, N.; Pulker, H. K. *Optical Interference Coatings*; Springer: Berlin, 2003.

(52) Cortie, M. B.; Dowd, A.; Harris, N.; Ford, M. J. *Phys. Rev. B* **2007**, *75*, 113405.